Mössbauer Spectra and Crystal Structure of Dinuclear Iron(II,III) Complex $[Fe_2(bpmp)(ena)_2](BF_4)_2$ of a Septadentate Polypyridine Ligand (Hbpmp): An Example of Fast Electron Interexchange

Yonezo MAEDA,* Yuichi TANIGAWA, Naohide MATSUMOTO, Hiroki OSHIO,†
Masatatu SUZUKI,†† and Yoshimasa TAKASHIMA#
Department of Chemistry, Faculty of Science, Kyushu University, Hakozaki, Higashiku, Fukuoka 812
†Department of Chemistry, Faculty of Science, Tohoku University, Aoba, Aramaki, Sendai 980
††Department of Chemistry, Faculty of Science, Kanazawa University, Kakumamati, Kanazawa 920
(Received July 29, 1993)

The Mössbauer spectra, magnetic susceptibilities, cyclic voltammograms, and electronic spectra of the dinuclear iron(II,III) complex, $[Fe_2(bpmp)(ena)_2](BF_4)_2$, were measured and the crystal structure was determined at 293 K, where Hbpmp represents 2,6-bis[bis(2-pyridylmethyl)aminoethyl]-4-methylphenol and Hena is heptanoic acid. The valence states of the irons of the complex are localized below about 200 K in the Mössbauer time scale (10^{-7} s), and are delocalized above 260 K. The activation energy of the electron interexchange between Fe^{2+} and Fe^{3+} was evaluated to be 15 kJ mol^{-1} at between 200 and 230 K based on an analysis of the Mössbauer spectra. The complex crystallizes in the monoclinic system, space group $P2/c$, with $a=10.129(4)$, $b=23.295(30)$, $c=11.324(7)$ Å, $\beta=104.55(4)°$, $d_{calc}=1.34$ g cm^{-3}, $Z=2$, and molecular formula $Fe_2F_8O_5N_6C_{47}B_2H_{59}$. The structure was solved by the heavy-atom method and was refined anisotropically by the least-squares method, employing 1981 unique reflections with $|F|>4\sigma(F_o)$.The hydrogen atoms of bpmp were located and refined by an isotropic approximation. The final R and R_w were 7.0 and 8.2%, respectively. The Fe–Fe distance was 3.365 Å, the average Fe–O value 2.033 Å, the average Fe–N value 2.188 Å, and the Fe–O–Fe angle 112.3(4)°. These values support the idea that both iron atoms are in an averaged valence state at 293 K.

The dinuclear iron centers in the active sites of metalloprotein play an important role in biological systems:[1] methane monooxygenase,[2] ribonucleotide reductase,[3] purple acid phosphatase,[4] and haemerythrin.[5] Model compounds using a variety of multidentate ligands have been prepared and characterized using various spectroscopic techniques.[6] The detrapped valence state of iron compounds in a solid has been observed in the system of ferrocene derivatives,[7,8] and $[Fe_3O(O_2CCH_3)_6L_3]L$ (L is a solvent molecule) using Mössbauer spectroscopy.[9] Ferrocene derivatives, which show a detrapped valence state even at 4.2 K, have recently been reported.[8] Iron complexes with a septadentate polypyridine ligand (Hbpmp) were synthesized by Suzuki et al.[10a,10b] and a bpmp complex with carboxylic acid having a long chain ($CH_3(CH_2)_7COOH$), which exhibits a detrapped valence state above 260 K, was reported by our group.[11]

The dynamical behavior of intervalence charge-transfer transitions in $[Fe_2(bpmp)(ena)_2](BF_4)_2$ is shown based on the Mössbauer spectra of the complex, and the character of the crystal structure of the complex is discussed in order to clarify the mechanism of an intramolecular electron transfer between metal atoms through bridged ligands.

Experimental

The complex was synthesized according to a method reported elsewhere.[10a,10b] Single crystals for X-ray analysis were obtained in acetonitrile.

Physical Measurements. The Mössbauer spectra for crystals of the complex were measured using a constant-acceleration spectrometer (Austin Science Associate). The data were stored in a 1024-channel analyzer (type 5200, Inotech Inc.). The temperature was monitored with a calibrated copper vs. constantan thermocouple within a variable temperature cryostat (type ASAD-4V, Austin Science Association). A cobalt-57 source of 10 mCi diffused into a palladium foil was used for the absorption measurement. The Mössbauer spectra were analyzed at the Computer Center of Kyushu University, and the velocity scale was normalized to an iron foil at room temperature.

The magnetic susceptibilities of the polycrystalline samples were measured by the Faraday method using an electrobalance (type 2002, Cahn Instrument) with an electromagnet (0.8 T). The temperature was controlled over 80—300 K using a digital temperature controller (model 3700, Scientific Instruments). $HgCo(NCS)_4$ was used as a calibration substance. The effective magnetic moment was calculated by the formula $\mu_{eff}=2.83\sqrt{\chi_M T}$, where χ_M is a molar susceptibility after applying diamagnetic corrections.

Cyclic voltammograms of the complex in acetonitrile (containing 0.1 M $(Bu_4N)ClO_4$ as supporting electrolyte) (1 M=1 mol dm^{-3}) were measured using an AC DC Cyclic Polarograph P-900 (Yanaco) at 295 K under an argon atmosphere. A standard three-electrode system comprising a glassy carbon working electrode, a saturated Ag/AgCl reference electrode, and a counter electrode of platinum was used for cyclic voltammetry experiments. Ferrocene was used as a standard substance.

The electronic spectra were recorded using a Shimadzu MPS-5000 spectrometer at room temperature.

Collection and Refinement of X-Ray Data for $[Fe_2(bpmp)(ena)_2](BF_4)_2$. Intensity data were obtained from a dark-green block (0.3×0.3×0.1 mm) which was placed on a Rigaku AFC5 four-circle diffractometer

#Present address: Kyushu Environmental Evaluation Association, Matsukadai, Higashiku, Fukuoka 812.

equipped with a Mo $K\alpha$ (0.71069 Å) source and a graphite monochrometer. Preliminary diffractometer routines indicate a monoclinic cell with space group $P2/c$, and lattice constants $a=10.129(4)$, $b=23.295(30)$, $c=11.324(7)$ Å and $\beta=104.55(4)°$ as determined from 20 selected reflections. The volume of the unit cell is 2661.56(0) Å^3 with $Z=2$. The crystallographic data for the complex are listed in Table 1.

A total of 3312 data was collected with the ω–2θ scan, yielding 1981 reflections with $|F|>4\sigma>(F_o)$ for the analysis. There was no variation in the intensities of the standard reflections during data-collection. Although the intensity data were corrected for both Lorentz and polarization factors, they were not collected for either absorption or extinction.

The structure was solved by a conventional heavy-atom method, and refined by a full-matrix least-squares method with anisotropic thermal parameters for non-hydrogen atoms and isotropic for hydrogen atoms. The weighting scheme $w=[\sigma^2+(0.03|F_o|)^2]^{-1}$ was employed, where σ was estimated from the counting statistics. The final indices (R and R_w) were 7.0 and 8.2%, respectively, which are defined as $R=\Sigma(|F_o|-|F_c|)/\Sigma|F_o|$ and $R_w=[\Sigma w(|F_o|-|F_c|)^2/\Sigma w|F_o|^2]^{1/2}$. The scattering factors for non-hydrogen atoms were taken from Ref. 12 and those for hydrogen atoms from Stewart et al.[13] The effects of anomalous scattering for non-hydrogen atoms were corrected for in structure-factor calculations. A determination of the structural parameters was carried out with the universal crystallographic program using XTAL 3.2.[14] The final atomic coordinates for the cation and boron atoms are given in Table 2.

Table 1. Crystallographic Data for $[Fe_2(bpmp)(ena)_2](BF_4)_2$

Temperature/K	293
Formula	$Fe_2F_8O_5N_6C_{47}B_2H_{59}$
F.W.	1073.32
Crystal system	monoclinic
Space group	$P2/c$
a (Å)	10.129(4)
b (Å)	23.295(30)
c (Å)	11.324(7)
α/°	90
β/°	104.55(4)
γ/°	90
U (Å^3)	2661.56(0)
Z	2
D_c (g cm^{-3})	1.34
D_m (g cm^{-3})	1.37
Radiation (Mo $K\alpha$)	0.71073
Color	Dark green
Sample size (mm)	0.3×0.3×0.1
Diffractometer	Rigaku AFC5
Octant	$0<h<13$
	$0<k<29$
	$-14<l<14$
Max scan times	3
Scan speed (° min^{-1})	2
Scan method	ω–2θ
Total data	3312
Independent	1981($|F|>4\sigma|F_o|$)
R	7.0%
R_w	8.2%
Weight	$1/(\sigma^2+(0.03|F_o|)^2)$
GFO	1.738

Results and Discussion

Magnetic Properties. The magnetic susceptibility data obtained at 80—300 K were fitted by the equation derived from the general isotropic exchange Hamiltonian in a dinuclear system, $H=-2JS_1\cdot S_2$ ($S_1=2$ and $S_2=5/2$) and $g=2.10$,

$$\chi=\frac{N\beta^2g^2}{4kT}\cdot\frac{x^{24}+10x^{21}+35x^{16}+84x^9+165}{x^{24}+2x^{21}+3x^{16}+4x^9+5}+N\alpha,$$

where $x=\exp(-J/kT)$, the symbols have usual meaning, and the temperature-independent paramagnetisms ($N\alpha$) were assumed to be zero. The values of the magnetic moments for the complex were consistent with an isotropic magnetic-exchange interaction between high-spin Fe(II) and Fe(III) ions.[10a,10b] The value of $J=-0.9$ cm^{-1} evaluated for the complex suggests that the magnetic interaction between the iron atoms is very week

Table 2. Positional and Isotropic Displacement Parameters for All Atoms Except Hydrogen and Fluorine Atoms of $[Fe_2(bpmp)(ena)_2](BF_4)_2$ with Estimated Standard Deviations in Parentheses

Atom	x	y	z	B_{iso}
Fe	0.1709(1)	0.75912(5)	0.3017(1)	0.548(5)
O1	0	0.8076(4)	1/4	0.057(3)
O2	0.1400(7)	0.6981(3)	0.1711(6)	0.071(3)
O3	0.0808(7)	0.7088(3)	0.4087(6)	0.072(3)
N1	0.2521(7)	0.8275(3)	0.4389(6)	0.057(3)
N2	0.2628(7)	0.8176(4)	0.1980(7)	0.060(3)
N3	0.3606(7)	0.7223(4)	0.4094(7)	0.063(3)
C1	0.347(1)	0.8648(5)	0.393(1)	0.063(5)
C2	0.323(1)	0.7950(5)	0.5507(9)	0.069(5)
C3	0.137(1)	0.8637(5)	0.466(1)	0.067(5)
C4	0.3098(9)	0.8671(4)	0.257(1)	0.057(4)
C5	0.332(1)	0.9156(5)	0.196(1)	0.073(5)
C6	0.309(1)	0.9136(6)	0.070(1)	0.084(6)
C7	0.262(1)	0.8633(6)	0.009(1)	0.084(6)
C8	0.238(1)	0.8163(6)	0.077(1)	0.066(5)
C9	0.4114(9)	0.7490(4)	0.5166(8)	0.063(4)
C10	0.535(1)	0.7332(6)	0.590(1)	0.081(5)
C11	0.606(1)	0.6895(7)	0.558(1)	0.095(6)
C12	0.550(1)	0.6607(6)	0.450(1)	0.102(7)
C13	0.427(1)	0.6789(6)	0.378(1)	0.085(5)
C14	0	0.8682(6)	1/4	0.058(6)
C15	0.0658(9)	0.8969(4)	0.3562(9)	0.058(4)
C16	0.063(1)	0.9564(5)	0.352(1)	0.079(5)
C17	0	0.9875(7)	1/4	0.081(7)
C18	0	1.0559(6)	1/4	0.13(1)
C19	0.029(1)	0.6827(4)	0.0971(9)	0.063(4)
C20	0.030(1)	0.6329(5)	0.014(1)	0.090(5)
C21	−0.112(2)	0.6128(7)	−0.049(1)	0.156(9)
C22	−0.114(2)	0.564(1)	−0.128(2)	0.21(1)
C23	−0.255(3)	0.550(1)	−0.208(2)	0.25(2)
C24	−0.259(3)	0.492(2)	−0.280(3)	0.32(2)
C25	−0.357(4)	0.490(2)	−0.353(4)	0.35(3)
B1	0	0.755(1)	3/4	0.10(1)
B2	1/2	0.928(1)	3/4	0.12(2)

and, therefore, the exact sign of J should be determined by a measurement at low temperature. Analogous mixed-valence dinuclear iron(II,III) and manganese(II,III) complexes with phenolato and two carboxylato bridges show a comparable magnitude of the antiferromagnetic interaction ($J=-3$——-8 cm^{-1}).[10a,10b]

Cyclic Voltammetry and Electronic Spectra. Cyclic voltammetry of the complex in acetonitrile shows two quasi-reversible waves at -0.05 and 0.69 V vs. SCE (referenced from Ag/AgCl), which correspond to Fe(II)Fe(II)/Fe(II)Fe(III), *E1* and Fe(II)Fe(III)/Fe(III)Fe(III), *E2* couples, respectively. The comproportionation constant of the following reaction K was calculated based on a separation of the redox potentials of *E1* and *E2*, using

$$[Fe(II)/Fe(II)] + [Fe(III)/Fe(III)] \rightleftharpoons 2[Fe(II)/Fe(III)]$$
$$E2 - E1 = RT/F \cdot \ln K. \quad (1)$$

The value obtained for the complex is $K=5.5\times10^{12}$ at 20 °C, indicating that the complex is highly stabilized.

Figure 1 shows the reflection spectrum of the complex. The spectrum consists of two broad bands due to a phenolate-to-Fe^{3+} charge-transfer transition at 300—500 nm and an intervalence charge-transfer transition between the two iron centers at around 1300 nm. The absorption spectrum in acetonitrile was also measured; such bands were observed in these regions. This fact may show that the complex keeps a Fe(II,III) dinuclear structure in acetonitrile.

Mössbauer Spectra. The Mössbauer spectra for the complex were measured at various temperatures, and are shown in Fig. 2. The spectra comprise two quadrupole doublets at 78 K; iron(II) having an isomer shift of 1.12 mm s^{-1} (quadrupole splitting of 2.87 mm s^{-1}) and iron(III) having an isomer shift of 0.48 mm s^{-1} (quadrupole splitting of 0.51 mm s^{-1}) were observed in accordance with a high-spin Fe(II)–Fe(III) formulation. The absorption area ratio (iron(III)/iron(II))

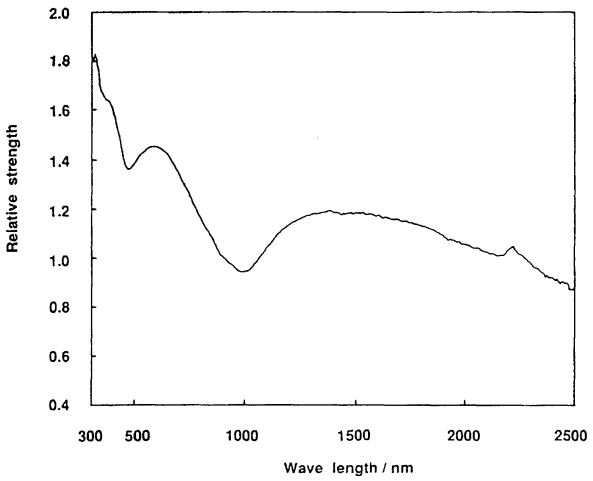

Fig. 1. Reflection spectrum of the complex.

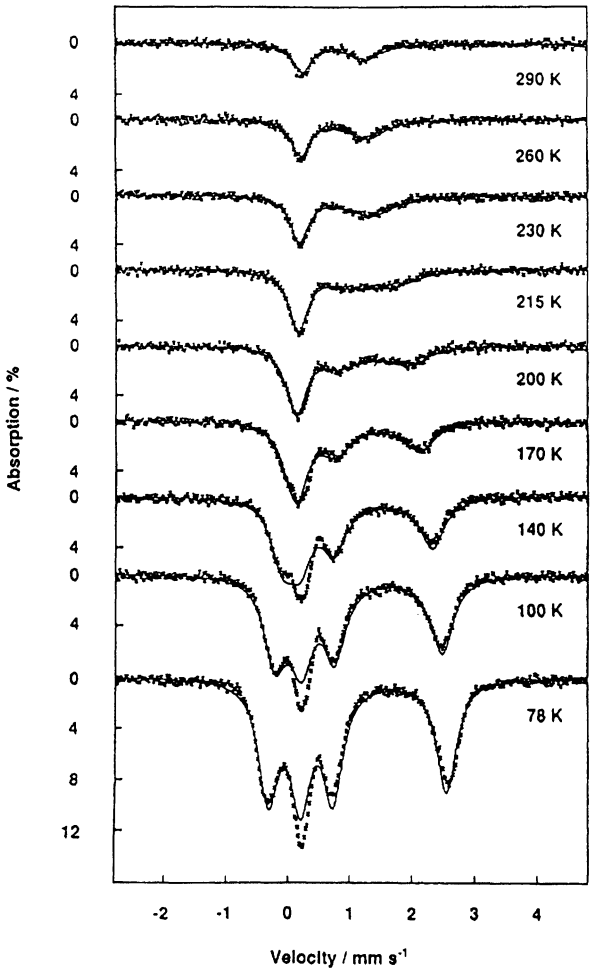

Fig. 2. Temperature dependences of the Mössbauer spectra for the complex and examples of the best fittings.

of 0.97 at 78 K was obtained. The spectrum at 290 K collapses into a doublet with Q.S.$=0.98$ mm s^{-1}, and the observed isomer shift value (0.70 mm s^{-1}) is on the average about 0.4—0.5 mm s^{-1} for high-spin iron(III) and about 0.9—1.0 mm s^{-1} for high-spin iron(II). The temperature dependences of the quadrupole splittings and the isomer shifts are shown in Figs. 3 and 4, respectively. The values of the quadrupole splittings for the Fe(II) and Fe(III) are observed to gradually approach each other along with increasing temperature, and fuse together at 230 K; such behavior is observed for the isomer shifts. These phenomena support the fact that the rates of electron interexchange between Fe^{2+} and Fe^{3+} become as fast as the inverse of the lifetime of the Mössbauer excited state. A similar behavior was also observed in mixed-valent biferrocenium complexes.[7,8] Curve fittings using the Wickman method[15] were carried out in order to determine the lifetime (τ) for which an iron atom is in a valence state. The best fits with the parameters listed in Table 3 are illustrated in Fig. 2. The temperature dependence of the quadrupole splitting for $Fe^{2+}$was taken into consideration under refer-

Table 3. Mössbauer Parameters Used in the Simulation and Lifetime Measured for $[Fe_2(bpmp)(ena)_2](BF_4)_2$

T/K	A/mms^{-1}	B/mms^{-1}	C/mms^{-1}	D/mms^{-1}	Red	τ/s
78	−0.315	0.225	0.735	2.555	3.46	6.1×10^{-6}
100	−0.245	0.230	0.730	2.465	2.64	2.5×10^{-6}
140	−0.150	0.225	0.715	2.310	1.90	1.6×10^{-6}
170	−0.020	0.225	0.715	2.140	1.32	8.7×10^{-7}
200	0.040	0.220	0.700	2.040	1.02	4.2×10^{-7}
215	0.080	0.225	0.695	1.980	0.86	2.3×10^{-7}
230	0.110	0.220	0.680	1.930	0.66	1.3×10^{-7}
260	0.155	0.220	0.670	1.845	0.50	9.5×10^{-8}
290	0.210	0.220	0.670	1.750	0.38	7.9×10^{-8}

A: Position of the lower energy peak of iron(II), B: Position of the lower energy peak of iron(III), C: Position of the higher energy peak of iron(III), D: Position of the higher energy peak of iron(II), Red: Reduction parameter of absorption strength for curve fitting, τ: Lifetime which an iron atom keeps in a valence state.

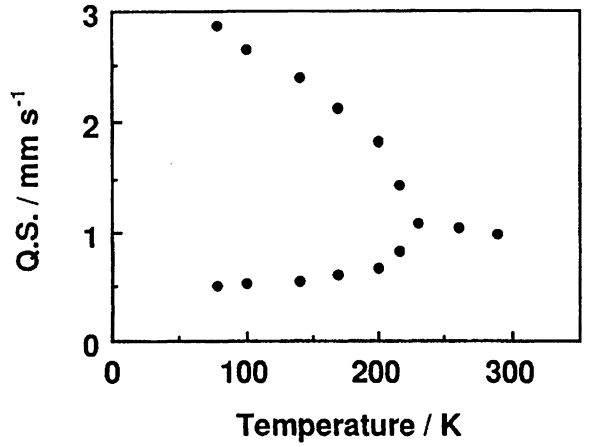

Fig. 3. Temperature dependence of the quadrupole splitting for the complex.

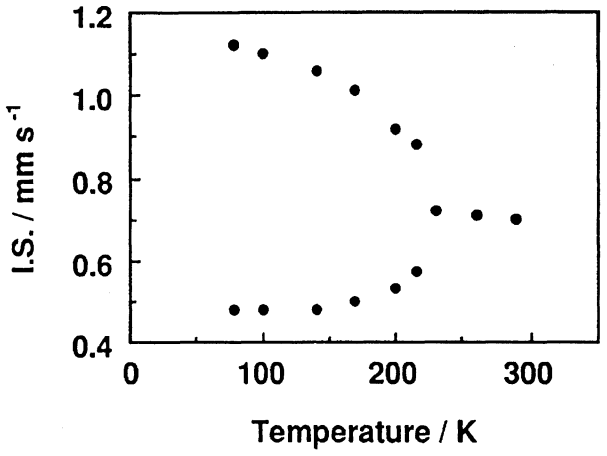

Fig. 4. Temperature dependence of the isomer shift for the complex.

ence of the Mössbauer parameters for $[Fe_2(bpmp)(isobutylic\ acid)_2](ClO_4)_2$, which does not show the averaged valence state over the 78—298 K temperature range. The deviations in the theoretical curves from the observations at low temperature are due to a relaxation of high-spin iron(III). The unsymmetric doublet of the Mössbauer spectrum observed at 290 K is properly revealed in the theoretical curve, and synmmetrical doublets must appear if the rate of electron interexchange becomes much faster than the inverse of the lifetime of the Mössbauer excited state. Plots of the natural logarithm of the lifetime evaluated for the complex vs. $1/T$ are shown in Fig. 5, and an activation energy of 15 kJ mol^{-1} was evaluated at between 200 and 230 K.

The temperature hysteresis effect in the transition rate was observed, suggesting that the transition of the trapped-to-detrapped valence state is accompanied by a phase transition. It is reported that a phase transition accompanying the motion of solvents contained in the crystals plays an important role in the change of the electron interexchange rate for trinuclear mixed-valence iron acetate complexes.[16]

X-Ray Structure. The crystal structure of the complex was determined at 293 K. Selected bond lengths and angles for a cation are listed in Table 4. The coordinates of the anions and hydrogen atoms and the other bond lengths and angles for the complex can be found in supplementary materials. The coordinates of the hydrogen atoms for heptanoic acid were not calculated, because the thermal factors of the carbon atoms of heptanoic acid were very large. Since the positions of the fluorine atoms of the anions were not clear, eight fluorine atoms for one BF_4^- were located and the crystal structure was determined. The structure of a cation is given in Fig. 6. A C_2-axis is present in the O1–C14–C17–C18 axis. Both of the iron atoms in the complex form a six-coordinated octahedron of the N_3O_3 type, and are bridged with a phenolate and two carboxylates. Two iron atoms are equivalent, and an average Fe–N value of 2.188 Å and an average Fe–O value of 2.033 Å were found. The average Fe–O bond lengths are intermediate between the Fe(II)–O and Fe(III)–O values, of which data support that both of the iron atoms are in an averaged valence state. The Fe–Fe distance and Fe–

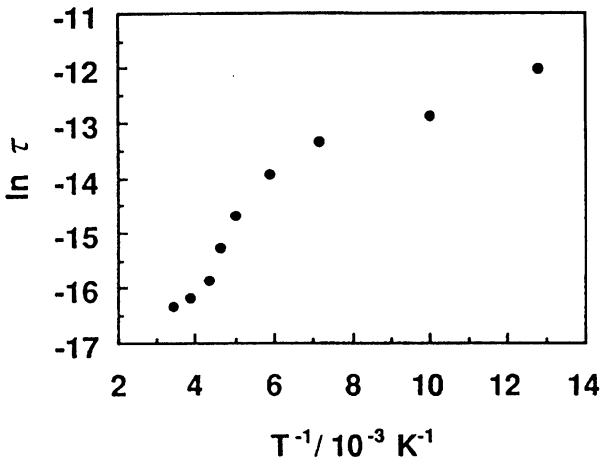

Fig. 5. Plots of the natural logarithm of the lifetime vs. $1/T$ for the complex.

Table 4. Selected Bond Lengths (Å) and Angles (deg.) for $[Fe_2(bpmp)(ena)_2](BF_4)_2$[a)]

	a. Bond lengths		
Fe–Fe	3.365(7)	Fe–O1	2.026(5)
Fe–O2	2.018(6)	Fe–O3	2.056(7)
Fe–N1	2.233(7)	Fe–N2	2.156(9)
Fe–N3	2.176(7)	O1–C14	1.41(2)
O2–C19	1.27(1)	O3–C19	1.26(1)
N1–C1	1.48(1)	N1–C2	1.50(1)
N1–C3	1.53(1)	N2–C4	1.36(1)
N2–C8	1.33(1)	N3–C9	1.35(1)
N3–C13	1.31(2)	C19–C20	1.49(2)
	b. Bond angles		
O1–Fe–O2	102.5(2)	O1–Fe–O3	90.8(2)
O1–Fe–N1	86.7(2)	O1–Fe–N2	86.9(2)
O1–Fe–N3	162.1(2)	O2–Fe–O3	91.2(3)
O2–Fe–N1	167.0(3)	O2–Fe–N2	93.1(3)
O2–Fe–N3	94.9(3)	O3–Fe–N1	97.9(3)
O3–Fe–N2	175.5(3)	O3–Fe–N3	84.6(3)
N1–Fe–N2	78.1(3)	N1–Fe–N3	76.8(3)
N2–Fe–N3	96.5(3)	Fe–O1–C14	123.9(2)
Fe–O1–Fe	112.3(4)	Fe–O2–C19	129.1(7)
Fe–O3–C19	139.9(6)	Fe–N1–C1	109.5(6)
Fe–N1–C2	104.0(6)	Fe–N1–C3	111.5(5)
C1–N1–C2	112.0(8)	C1–N1–C3	110.1(8)
C2–N1–C3	109.6(8)	Fe–N2–C4	114.4(7)
Fe–N2–C8	123.3(7)	C4–N2–C8	118.7(9)
Fe–N3–C9	114.0(6)	Fe–N3–C13	126.1(7)
C9–N3–C13	119.8(8)	O1–C14–C15	118.7(6)
C15–C14–C15	123(1)	O2–C19–C20	120(1)
O2–C19–O3	121.3(9)	C20–C19–O3	119.1(9)

a) Estimated standard deviations in the least significant digits are given in parentheses.

O–Fe angle are 3.365 Å and 112.3°, respectively; those values are comparable to 3.365 Å and 113.1° found for $[Fe_2(bpmp)(OPr)_2](BPh_4)_2$ determined by Borovik and Que,[17] respectively. For a comparison, $[Fe_2(bpmp)(OPr)_2](BPh_4)_2$ belongs to a triclinic $P\bar{1}$ space group and the averaged Fe(1)–O (2.088 Å) and Fe(1)–N (2.174 Å) bond lengths are longer than the averaged Fe(2)–O

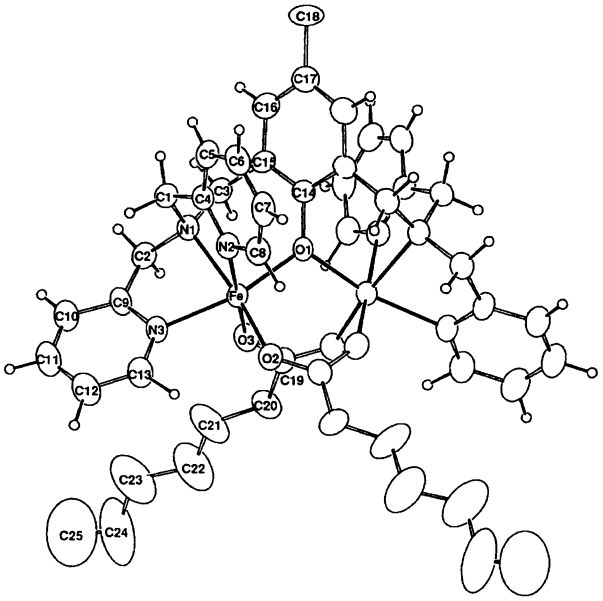

Fig. 6. Ortep drawing for a $[Fe_2(bpmp)(ena)_2]^{2+}$ cation.

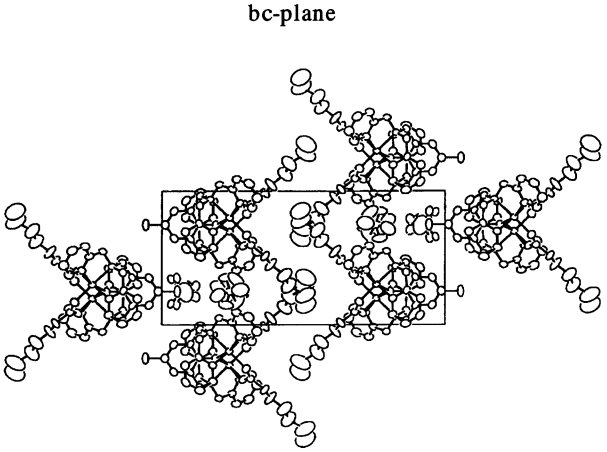

Fig. 7. Packing diagram in the bc-plane for the complex.

(1.957 Å) and Fe(2)–N (2.156 Å), respectively, where Fe(1) is divalent and Fe(2) is trivalent.

A packing diagram of the complex is shown in Fig. 7. Since the anisotropic thermal parameters of the terminal carbon atoms of the heptanoic acids are very large, the methylene chains of the heptanoic acids constitute a quasi-amorphous layer. A statistical disorder is found in the anion sites; an anion has two sites which are very close each other (ca. 0.3 Å).

It has been communicated that the onset of motion of a ligand or a solvent molecule affects the rate of electron transfer in the case of trinuclear mixed valence iron acetate complexes, and that electron delocalization in biferrocenium triiodide accompanies the motion of the counter ions.[17] Sano et al. have reported very recently that an analogous trinuclear iron complex with carboxylic acid with a long chain shows a delocalized valence state and a non-linearity of $\ln[A(T)/A(78)]$, (A

is Mössbauer absorption area).[18]

We have reported that bpmp complexes with carboxylic acid having a longer chain than valeric acid ($CH_3(CH_2)_3COOH$) show a rapid intervalence charge-transfer transition.[19] It seems to be important in understanding a rapid electron interexchange that the atoms of the tail part of heptanoic acid have a large temperature factor, and that there is large space in the layer formed by two heptanoic acids (Fig. 7).

Supplementary Materials are Available: Tables of Positional and Isotropic Displacement Parameters for All Atoms Except Some Hydrogen Atoms, Anisotropic Thermal Parameters of Atoms Except Hydrogen Atoms, Bond Lengths (Å) and Bond Angles, Packing Diagrams in ac- and ab-Planes, and the Observed and Calculated Structure Factors for $[Fe_2(bpmp)(ena)_2](BF_4)_2$ are deposited as Document No. 67001 at the Office of the Editor of Bull. Chem. Soc. Jpn.

The authors wish to thank Dr. Masahiko Suenaga for assisting in the preparation of the sample.

References

1) P. C. Wilkins and R. G. Wilkins, *Coord. Chem. Rev.*, **79**, 195 (1987), and references cited therein.

2) M. P. Woodland, D. S. Patil, R. Cammack, and H. Dalton, *Biochim. Biophys.*, **873**, 237 (1986).

3) B. M. Sjoberg and A. Graslund, *Adv. Inorg. Biochem.*, **5**, 47 (1983).

4) B. C. Antanaitis and P. Aisen, *Adv. Inorg. Biochem.*, **5**, 111 (1983).

5) a) R. G. Wilkins and P. C. Harrington, *Adv. Inorg. Biochem.*, **5**, 51 (1983); b) P. C. Wilkins and R. G. Wilkins, *Coord. Chem. Rev.*, **79**, 195 (1987).

6) a) D. M. Kurtz, Jr., *Chem. Rev.*, **90**, 585 (1990), and references cited therein; b) A. S. Borovik, B. P. Murch, L. Que, Jr., *J. Am. Chem. Soc.*, **109**, 7190 (1987); c) S. Menge, Y. Zang, M. P. Hendrich, and L. Que, Jr., *J. Am. Chem. Soc.*, **114**, 7786 (1992); d) K. J. Oberhausen, J. F. Richardson, R. J. O'Brien, R. M. Buchanan, J. K. Webb, and D. N. Hendrickson, *Inorg. Chem.*, **31**, 1125 (1992).

7) D. O. Cowan, C. LeVanda, J. Park, and F. Kaufman, *Account Chem. Res.*, **6**, 1 (1973).

8) a) W. H. Morrison, Jr., and D. N. Hendrickson, *J. Chem. Phys.*, **59**, 380 (1973); b) S. Nakashima and H. Sano, *Bull. Chem. Soc. Jpn.*, **62**, 3012 (1989).

9) a) M. Sorai, A. Nishimori, D. N. Hendrickson, T. -Y. Dong, and M. J. Cohn, *J. Am. Chem. Soc.*, **109**, 4266 (1987); b) M. Konno and H. Sano, *Bull. Chem. Soc. Jpn.*, **61**, 1455 (1988); c) C. T. Dziobkowski, J. T. Wrobleski, and D. E. Brown, *Inorg. Chem.*, **20**, 679 (1980).

10) a) M. Suzuki, A. Uehara, H. Oshio, K. Endo, M. Yanagi, S. Kida, and K. Saito, *Bull. Chem. Soc. Jpn.*, **60**, 3547 (1987); b) M. Suzuki, H. Oshio, A. Uehara, K. Endo, M. Yanaga, S. Kida, and K. Saito, *Bull. Chem. Soc. Jpn.*, **61**, 3907 (1988).

11) Y. Maeda, Y. Tanigawa, S. Hayami, and Y. Takashima, *Chem. Lett.*, **1992**, 591.

12) J. A. Ibers and W. C. Hamilton, "International Tables for X-Ray Crystallography," Kynoch Press, Birmingham, England (1974), Vol. IV.

13) R. F. Stewart, E. R. Davidson, and W. T. Simpson, *J. Chem. Phys.*, **42**, 3175 (1965).

14) S. R. Hall and J. M. Stewart, University of Western Australia and Maryland:Nedlands, Australia and College Park MD, 1992.

15) H. H. Wickman, "Mössbauer Effect Methodology," ed by I. J. Gruverman, Plenum Press, New York (1966), p. 39.

16) a) S. Nakashima, Y. Masuda, I. Motoyama, and H. Sano, *Bull. Chem. Soc. Jpn.*, **60**, 1673 (1987); Y. Masuda and H. Sano, *Bull. Chem. Soc. Jpn.*, **60**, 2674 (1987); b) M. Sorai and D. N. Hendrickson, *Pure Appl. Chem.*, **63**, 1503 (1991).

17) A. S. Borovik and L. Que, *J. Am. Chem. Soc.*, **110**, 2345 (1988).

18) T. Nakamoto, M. Katada, and H. Sano, *Chem. Lett.*, **1991**, 1323; **1990**, 225.

19) Y. Maeda, Y. Tanigawa, Y. Ando, Y. Takashima, and N. Matsumoto, *Acta Chim. Hung., Models in Chemistry*, **130**, 55 (1993).